

RESEARCH ARTICLE

Optical design of a tunable microneedle array for photodynamic therapy of metastatic melanomas

Diptayan Dasgupta ^a, Sonam Berwal ^{b,c}, Bharpoor Singh ^b, Neha Khatri ^{b,c*}

^a Department of Applied Optics and Photonics, University of Calcutta, Kolkata 700106, India

^b CSIR-Central Scientific Instruments Organisation, Chandigarh 160030, India

^c Academy of Scientific & Innovative Research (AcSIR), Ghaziabad 201002, India

* Corresponding author's Email: nehakhatri@csio.res.in

© The Author(s), 2024

Abstract

The need for photodynamic therapy is increasing with the rise of skin cancer melanoma detection. However, low penetration depth of light in the UV range and higher scattering of skin tissues cause harsh clinical practices and reduced irradiance for the activation of chemicals such as photosensitizers to facilitate cell necrosis of malignant tumors. In this paper, a tunable microlens integrated on a microneedle array is designed for variable focusing to reduce melanomas at multiple sites with an improved intensity for reactive oxygen species production. A light distribution of 36% percent of the input intensity is achieved at the targeted distance of 4.35 mm for blue light. Red light attained a light distribution of 13% of the input intensity at a targeted distance of 6.5 mm. Designing such a light, delivery-based in-vivo biomedical device is of extreme importance for photodynamic therapy of skin cancer on and beyond the epidermal tissue layer.

Keywords: Microneedle array, microlens, skin cancer, target delivery, optical design

Article history:

Received: 01-July-2023

Revised: 13-Oct-2023

Accepted: 07-Nov-2023

1. Introduction

Cancer is a major public health issue on a global scale, as evidenced by the 10 million deaths caused in 2020 (Sung et al., 2021). Amongst all the types of cancers found in the human body, skin cancer is one of the most aggressive and lethal forms of cancer that pose a significant threat to public health due to its ability to resist chemotherapy and spread to other parts of the body through metastasis. Based on its origin and certain medical characteristics, skin cancer can be classified into three general types which include basal cell carcinomas, squamous cell carcinomas, and cutaneous melanomas (Naidoo, Kruger, & Abrahamse, 2018). Basal cell carcinomas and squamous cell carcinomas are classified as nonmelanocytic skin cancers, and they do not typically spread to adjacent healthy tissues (Allen, 2000). In contrast, cutaneous melanomas are considered to be metastatically invasive, as they can spread and infect nearby healthy tissues (Eggermont et al., 2014). Being known to be highly drug-resistant, cutaneous melanomas cause low patient survival and a high rate of relapse. Cutaneous Melanomas usually result from the malignancy of a single melanocyte or the malfunctioning of dysplastic nevi, which are cells responsible for producing the melanin pigment and are located in the deepest regions of the epidermis and the early regions of the dermis (Naidoo et al., 2018). As skin cancer progresses, metastatic melanoma develops when cancerous cells from the epidermis spread and invade distant organs in the body. As of today's date, more than 80% of skin cancer deaths are caused due to metastatic melanomas (Paluncic et al., 2016).

Photodynamic therapy (PDT) is an immensely crucial method for the treatment of metastatic melanomas (Naidoo et al., 2018). The procedure involves a dynamic interaction between photosensitizer (PS), reactive oxygen species

(ROS), and light. PS can be classified into four basic types, which include porphyrins, phthalocyanines, chlorins and porphycenes (Abrahamse & Hamblin, 2016). Porphyrins are excessively used for PDT applications as they are known to be very much stable whereas Phthalocyanines have higher PDT efficacy as they consist of a diamagnetic metal ion. (Jiang, Shao, Yang, Wang, & Jia, 2014; Singh et al., 2015). Chlorins have a higher PDT efficacy for basal cell carcinomas and squamous cell carcinomas (Calixto, Bernegossi, De Freitas, Fontana, & Chorilli, 2016). Porphycenes are isomeric structures of porphyrins but electronically configured (Ruiz-González et al., 2013). As depicted in **Fig. 1**, the PS in action forms a light-sensitive reaction to the targeted cancer cell which gets activated by the localization of light at a suitable wavelength resulting in the formation of cyto-toxic ROS, including singlet molecular oxygen, hydroxyl radicals, and superoxide anions. ROS induces photo cytotoxicity by subjecting cancer cells to oxidative stress, leading to the damage of their cellular biomolecules, such as lipids, proteins, and nucleic acids, and causing them to become inactive. This form of treatment is usually less invasive than conventional forms as it targets specific cancerous tumor regions based on their stage and causes limited side effects (Naidoo et al., 2018).

Efficient delivery of photosensitizers and therapeutic light is a critical requirement for effective photodynamic therapy. However, current delivery methods, such as intravenous injection of photosensitizers or direct illumination of the skin, have limitations. Intravenous injection can cause photosensitizer accumulation in the circulatory system, leading to harmful effects on healthy tissues (Zhao et al., 2022). Light delivery inside the skin tissue is also limited due to its scattering and absorption. Hence most of the studies for such applications are based on microneedle array (MNA) (M. Kim et al., 2016). MNAs are invasive tools that pierce through the stratum corneum to deliver drugs. The functionality of MNAs can be classified into two applications: Light-delivery MNAs and Drug Delivery MNAs (Ganeson et al., 2023; Li, Zhao, Zhang, Ling, & Zhang, 2022).

Despite the advantages of MNA-mediated transdermal delivery of photosensitizers having been proved, the delivery method of the other PDT key element, therapeutic light, is yet to be improved. For example, most of the clinical practices of PDT use direct application of the light source onto the skin tissue causing very high scattering and absorption inside the stratum corneum, hence reducing effectiveness (Kim & Darafsheh, 2020). Furthermore, the penetration depth of the UV light spectrum is on the lower end, such as for blue light, it is 1 mm and for red light, it is 4 mm (Ash, Dubec, Donne, & Bashford, 2017). As a result, limitations of the photosensitizer effectivity for metastatic melanomas occur in depths even more than 4 mm into the skin tissue. The spectral range spanning from 600 to 1200 nm is commonly referred to as the "optical window of tissue". However, it should be noted that light with wavelengths beyond 800 nm is incapable of producing singlet oxygen due to its insufficient energy required to initiate a photodynamic reaction, as opposed to shorter wavelengths (Sharman, Allen, & Van Lier, 1999; Zhu & Finlay, 2008). Selecting an appropriate light source for Photodynamic Therapy (PDT) can be a challenging task since no single light source is universally optimal for all indications, even when employing the same photosensitizer (PS). Factors to consider when making this choice include PS absorption, the tumor location, size, accessibility and tissue characteristics of the affected area, cost, and size of the light source (Kim & Darafsheh, 2020).

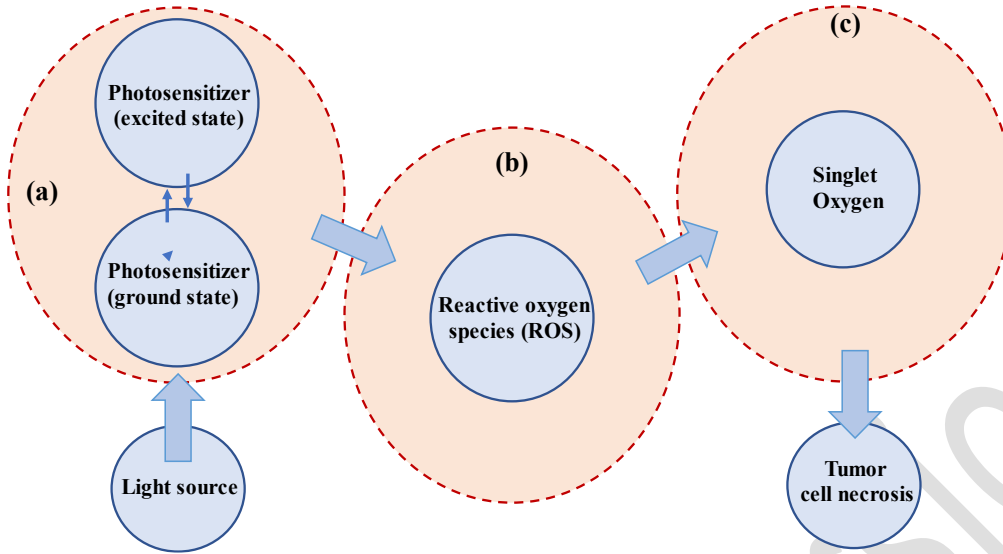


Fig. 1. Steps involved in photodynamic therapy. (a) Light is provided to the system which as a result activates the photosensitizer. (b) This indicated the production of ROS after the PS is excited. (c) Singlet oxygen, a type of ROS helps in the tumor cell necrosis procedure. When exposed to an appropriate wavelength, cancer cells undergo oxidative stress, inducing photo cytotoxicity through the formation of singlet molecular oxygen. This process damages cellular biomolecules like lipids, proteins, and nucleic acids, rendering the cancer cells inactive.

Several techniques to overcome the issue of light delivery and performance enhancement of light particles inside tissues have been reported. In 2016, Kim et al. first demonstrated the use of an optical lens-microneedle array (OMNA) to improve light delivery in human skin tissues at a wavelength of 498 nm, extending the penetration depth from 1.3 to 2.5 mm (Kim et al., 2016). In 2018, Wu et al. proposed a low-cost fabrication process for a painless and thinner structure of OMNA. They successfully demonstrated that OMNA could enhance the light transmission efficiency for light therapy (Wu, Kono, Takama, & Kim, 2019). They also designed a tunable thickness device consisting of a micropatterned optical sheet with MNA resulting in light transmission efficiency with reduced pain, and improved skin care in dermatology (Wu, Takama, & Kim, 2019). This led to the development of a height fixation device for blue light delivery on a culture dish and an LED system to conduct the cell apoptosis using an MNA array (Wu et al., 2022). Furthermore, Zhao et al. proposed a dual-function dissolvable MNA for delivering light as well as drugs with reduced therapeutic irradiance resulting in limited skin damage (Zhao et al., 2022). Yang et. al demonstrated a deep tissue light enhancement and delivery system for in vivo photothermal treatment, using gold nanoshells and a fabricated optical fiber needle array with multimodal fibers (Yang et al., 2017). The transportation of visible and near-infrared light to interstitial tissues has also been facilitated through the application of optical fibers and fiber-optic MNAs [(Guo et al., 2015; Okuno et al., 2013; Robinson et al., 2010)].

In this work, an optical design of a tunable microlens array integrated into a MNA array is proposed to address the therapeutic challenges associated with metastatic melanomas located in deep tissues beyond the epidermal layer. The design aims to have multiple focuses of light onto the skin tissue for multiple underlying tumors with enhanced light intensity distribution for blue and red light. It was developed to ensure compliance with the photothermal damage benchmark. Furthermore, an optimization method is also strategized for this application.

2. Design Methodology and Theoretical Formulation

In this section, the design methodology of the device is described with its theoretical formulation. Section 2.1 describes the human skin model design for this application. Section 2.2 shows the design principles of the microlens array (MLA) and MNA. The entire design procedure of the microlens array and microneedle array was performed using Zemax Opticstudio and Solidworks respectively.

2.1 Skin Model

The human skin is identified as an interfacial barrier from the environment. Light penetration inside skin tissue is different for different wavelengths. Blue light gets extinguished within 1 mm inside the tissue layer whereas it is

roughly around 4 mm for red light as shown in the schematic skin model in **Fig. 2**. The skin model has scattering properties which lead to light dispersion and hence, eventually reduces the energy density with increasing depth. The scattering model for photons inside tissues is designed using the Henvey-Greenstein scattering function (Ash et al., 2017):

$$P(\alpha) = \frac{1-g^2}{[1+g^2-2g\cos(\alpha)]^{\frac{3}{2}}} \quad (1)$$

where α is the longitudinal scattering function and g is the anisotropic factor, ranging from $-1 \leq g \leq 1$, from backscattering through isotropic scattering to forward scattering. The longitudinal scattering function is calculated by (Magnain, Elias, & Frigerio, 2008):

$$\alpha = \cos^{-1}\left\{\frac{1}{2g}\left[1 + g^2 - \left(\frac{1-g^2}{1-g+2gR}\right)^2\right]\right\} \text{ for } g \neq 0 \quad (2)$$

The thickness of each skin layer varies according to different body layers (Oltulu, Ince, Kokbudak, Findik, & Kilinc, 2018). The thickness of the skin affects the effectiveness of PDT in different regions of the body. Hence depending on the location, this can affect the diffusion of light and the absorption of the photosensitizing agent. The light diffusion flux is calculated using the below equation (Magnain et al., 2008):

$$\frac{df(u,\tau)}{d\tau} = -\frac{f(u,\tau)}{\mu} + \frac{\varpi}{4\pi|\mu|} \frac{F(u',\tau)}{|\mu'|} p(u,u') + \frac{\varpi}{4\pi|\mu|} \int_0^{4\pi} \frac{f(u_1,\tau)}{|\mu_1|} p(u,u_1) d\Omega_1 \quad (3)$$

where $\mu = \cos\Theta$ and $\varpi = s/(k+s)$. The scatterers embedded in the medium are characterized by their absorption and scattering coefficients, respectively, k and s . F , being the collimating flux, follows Fresnel and Snell's law. $P(\mathbf{u},\mathbf{u}_i)$ is defined as the phase function for probability for an incident light with the direction \mathbf{u}_i to be scattered in the direction \mathbf{u} . Single and multiple scattering are separated here and are respectively expressed by the second and third terms of equation (3).

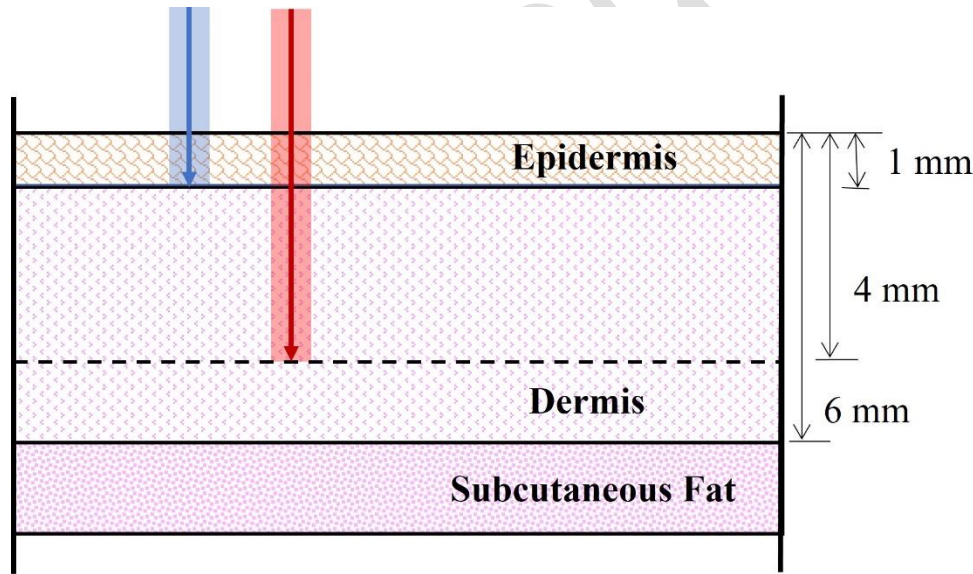


Fig. 2. Thickness model used for skin. Blue light cannot penetrate beyond 1mm inside the skin whereas red light can penetrate to 4mm inside the tissue.

The optical depth differential ($d\tau$) is factorized on parameters such as wavelength (λ), skin depth (z) and directions which are defined by angles (Θ, ϕ) and its unit vector \mathbf{u} . It is calculated by:

$$\int_0^z (k + s) dz \quad (4)$$

The incident angle is taken as 0° .

Table 1. Depth chart of skin for different body regions where PDT can be used (Oltulu et al., 2018).

Region	Epidermis (μm)	Dermis (μm)	Total Thickness (μm)
Breast	164.3	5888	6052.3
Scalp	112.4	3132.8	3245.8
Abdomen	163.3	5497.7	5661
Back	116	5717.8	5834
Dorsum of hand	244.8	2538.5	2284
Dorsum of foot	206.4	2363.3	2583

The dermis contains various sublayers including the upper blood net, reticular dermis and subcutaneous fat. The average depth chart of skin tissue for different body regions where this model can be used is shown in **Table 1**. The tumor size underneath the skin layers is classified according to the Breslow depth which is a helpful measure of how far melanoma has invaded the body (Marghoob, Koenig, Bittencourt, Kopf, & Bart, 2000). The staging of skin cancer melanomas can be classified into 9 levels starting from a depth of less than 0.76 mm, which makes the melanoma on site to distant metastasis (Iqbal, Biermann, Ali, Zaini, & Metzger, 2019; Keung & Gershenwald, 2018; Marghoob et al., 2000). Metastasis describes the spread of melanoma throughout the human skin to other parts of the body. M0, the earliest stage, denotes no evident distant metastasis whereas M1 metastasis denotes evident spread or distant metastasis. It is the last stage or stage IV of melanoma, which can occur at a depth of more than 4mm into the tissue. Usually, it means that the melanoma has proliferated the whole body.

PDT dosimetry also plays a crucial role in reducing melanoma and inducing cell necrosis (Naidoo et al., 2018; Swavey & Tran, 2013). This process is complex, as it involves the dynamic interactions of light, photosensitizer, and oxygen. The clinical efficacy of PDT is determined by multiple factors, such as the type of dosimetry employed, the total dose, light exposure time, delivery method, and fractionation scheme. Furthermore, the characteristics of the cancer type, melanoma spread, and skin thickness must also be taken into account (Kim & Darafsheh, 2020). Skin contains various chromophores with scattering and absorption coefficients that strongly depend on the wavelength of light. The tissue's scattering properties result from inherent chromophore attenuation and the size of particles within the tissue, which dictate the type of scattering that takes place. This scattering phenomenon causes light dispersion within the tissue, leading to a gradual reduction in energy density as depth increases (Ash et al., 2017).

2.2 Microlens and Microneedle Design

The proposed design consists of an 11x11 array of multifocal microlens and MNA where each microlens corresponds to an MNA structure. As depicted in **Fig 3a**, the variation of focal length is constructed in a vertical direction to focus on the subsequent layers of the skin tissue. The proposed MNA makes the light focus on multiple tumors, increasing the effective ROS formation and the accuracy of tumor reduction & elimination for PDT considering there is enough photosensitizer and ROS present in the tissue. The focal length of the MLA makes the illumination area tunable as shown in Fig. 3b. Increasing the field of illumination (FOI) results in a corresponding increase in the spread of light throughout the skin tissue. The designed MLA and MNA structure is useful for melanomas or tumors which occur at a depth of more than 3 cm, where blue and red light tend to get extinguished or have limited performances. The microlens array is designed using the following equation (Khatri, Berwal, Manjunath, & Singh, 2023):

$$R = (k + 1) \frac{h_L}{2} + \frac{r^2}{2h_L} \quad (5)$$

Where r is the lens distance concerning the optics axis and hL is the lens height at the vertex. For spherically designed MLA, $k=0$. The radius of curvature (R) relates to the focal length using the following equation:

$$f = \frac{R}{n(\lambda)-1} \quad (6)$$

Table 2. Microlens Array Dimensions.

Microlens array	Radius of Curvature (mm)	Back focal length (mm)
R1	1.3	2.51
R2	1.5	2.90
R3	1.7	3.29
R4	1.9	3.67
R5	2.0	3.87
R6	2.2	4.25
R7	2.4	4.64
R8	2.6	5.03
R9	2.8	5.41
R10	3	5.80
R11	3.25	6.28

The variable focal length helps in a better distribution of light radiation inside the skin tissue. The target design specification of the MLA is listed in **Table 2**. The R1-R11 is the specific row number for which the tunable focal length is presented. The proposed MLA and MNA can be produced as a single optical element using transparent and durable materials that do not harm the skin upon application. To fulfill this criterion, poly-lactic acid (PLA) is used as a suitable option for the MNA due to its refractive index of 1.47 and low absorption coefficient of 0.014 mm^{-1} for wavelengths beyond 400 nm. **Fig. 4 and 5** show the structure of the designed device. The selected light sources are two lasers with a wavelength of 491 nm and 675 nm with 20 mW power. To achieve optimal results with PDT, it is crucial to ensure the light source is suitable for the target tissue, delivery device, and photosensitizer. Laser technology is commonly employed for PDT due to its ability to generate coherent, monochromatic light with a narrow bandwidth. The exceptional optical power of lasers and their capacity to produce specific wavelengths make them an excellent choice for matching with particular photosensitizers (Kim & Darafsheh, 2020).

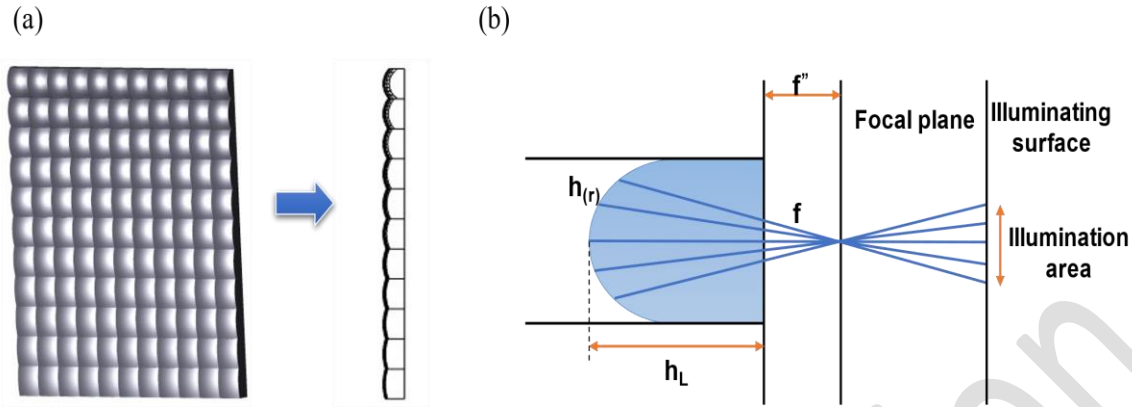


Fig. 3. (a) Variation of the tunability is constructed in the vertical direction. The lenses which appear to be thicker are short focusing whereas the thinner ones are longer focusing microlens. (b) The focal length is also a factor for the total field of illumination.

The needle inserts a force of about 2.75-2.8N which can be calculated by the buckling equation (He, Chen, & Tang, 2008):

$$P_e = \frac{\pi^2 EI}{4L^2} + \frac{\mu L^2}{\pi^2} \quad (7)$$

The maximum or critical force (P_e) is determined by the modulus of elasticity (E), area moment of inertia (I), column length (L), and spring constant (μ).

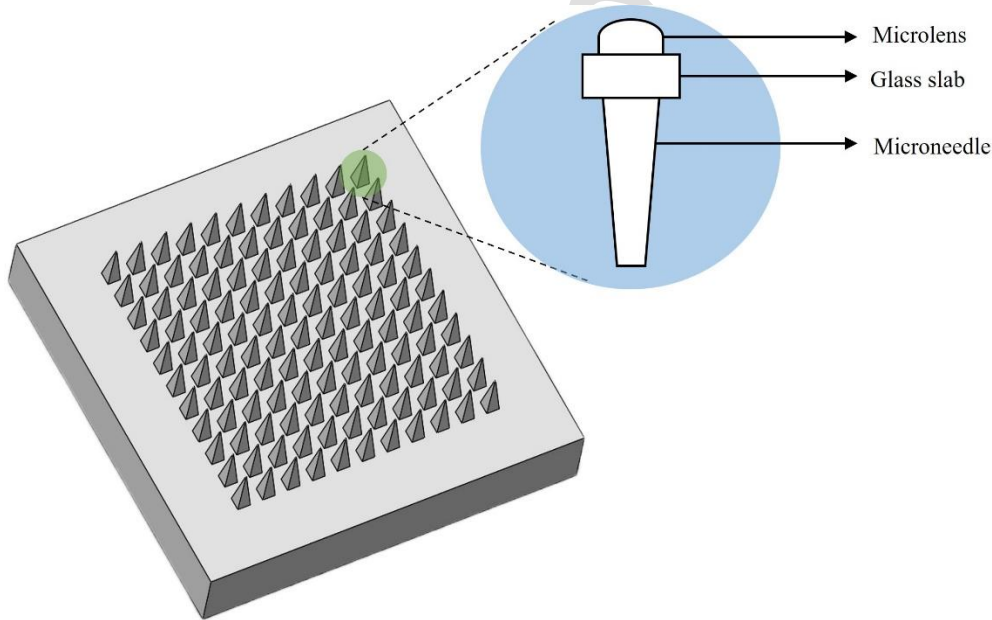


Fig. 4. Close view of the designed microlens integrated on a microneedle array structure.

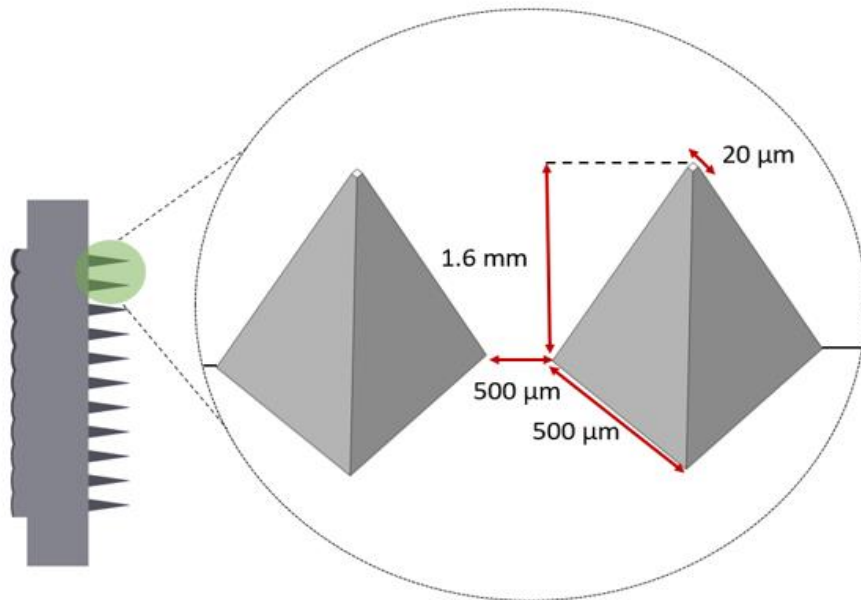


Fig. 5. Design parameters of the microneedle array for the field of view enhancement.

3. Computational Optimization and Simulation Results

In this section, the results obtained from this simulation study have been explained, along with an optimization strategy. Section 3.1 depicts the overall optimization procedure whereas section 3.2 depicts the results obtained.

3.1 Optimization Strategy

An optimization procedure has been shown to maximize performance, as illustrated in **Fig. 6**. The focusing depth is set primarily as the light on each layer of skin will depend on it. Modulating factors are then defined to set up the optimization pathways. This is solely dependent on the application and designated wavelength selection. The wavefront control system is designed to enable control of illumination using a ray mapping technique, depending on tissue constraints, thereby improving accuracy in the dosimetry of the photosensitizer. To achieve optimal penetration depth, a positional optimization system has been employed to design and set design constraints. Two sets of wavelengths, as mentioned earlier, have been considered to enhance penetration depth under realistic boundary conditions. Boundary conditions can be added based on the selection criteria of light dosimetry and spatial uniformity of the FOI. The larger the FOI, the more area is covered. Initially, a system with variable illumination space is obtained. Under this system, the optimization takes place through two pathways. The microlens with the lowest and the highest focal length values contribute to the limits of depth of field. Next, ray mapping is performed to point rays at every skin layer, keeping in mind the absorption rate of the tissue. The positional optimization system is used after ray mapping in order to find the limits of the rays. It usually gets reduced with the increase in skin depth. However, the FOI increases, providing a more diffused area of illumination, resulting in the reduction of light intensity. After that, the following step requires the checking of appropriate wavelength and field angles. Upon satisfying the parameters, the system gives optimized results. Otherwise, initial parameters are revised and the optimization method is performed again.

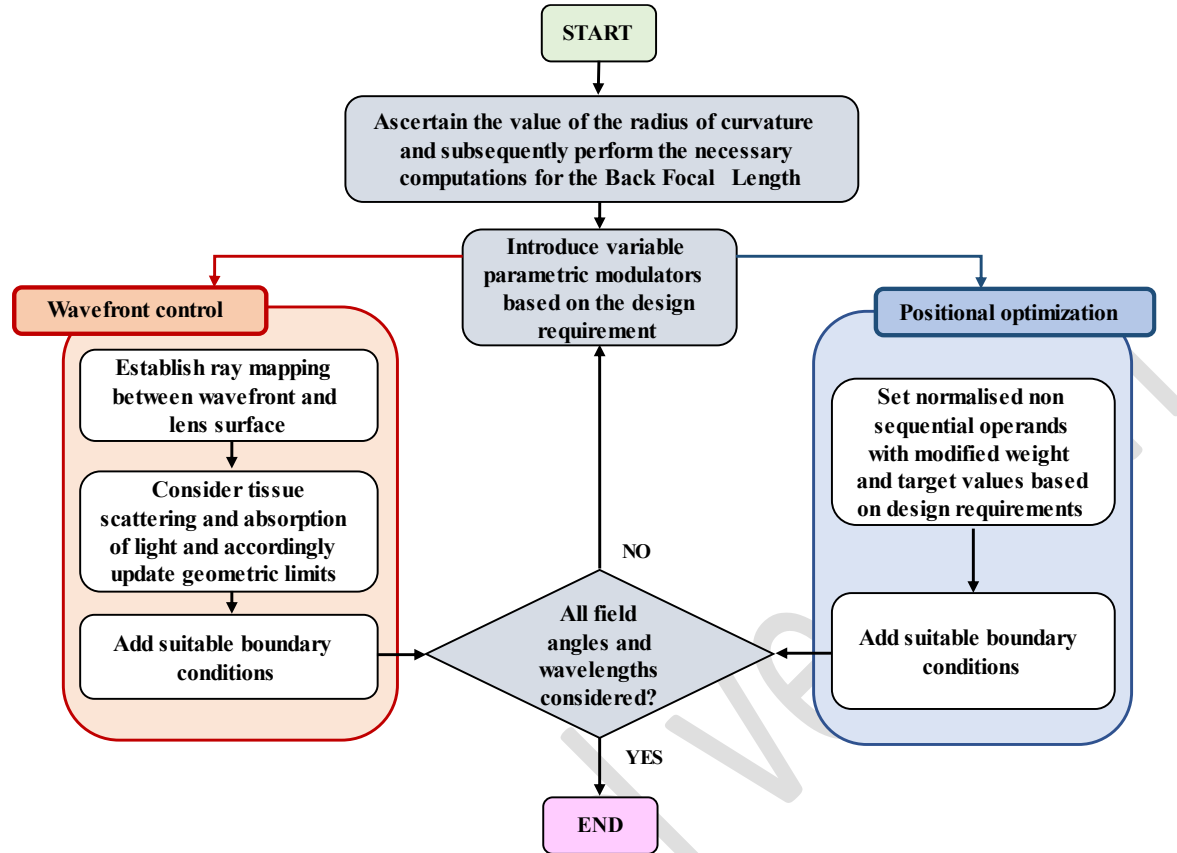


Fig. 5. Optimization algorithm flowchart to maximize the performance variables

4. Results and Discussion

The input laser strikes on the microlens array produce one beam for each needlepoint in an 11x11 system. The MNA acts as a bridging pathway device between air and high diffusion & absorption-enabled skin medium. Insertion of the MNA is a painless procedure, making the photodynamic process hassle-free with improved performance. **Fig. 7** shows the working principle of the variable focal length system. **Fig. 7a** denotes the microlens array schematics used for design whereas **Fig. 7b** denotes the variable illumination scheme after adding the microneedle array. Simulations were performed on the designed 11x11 array.

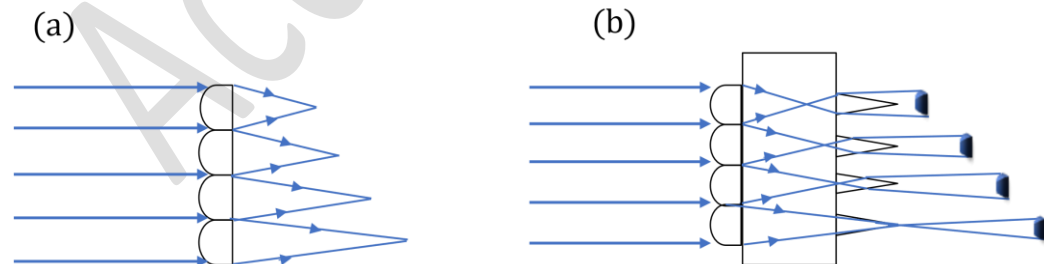


Fig. 7. (a) schematic of the working principle of a smaller tunable microlens array. (b) Schematics of the working principle of a smaller proposed design.

The microlens array has a distributed focusing scheme on the MNA for light penetration at different depths. This results in ROS production at different skin depths. The targeted depth for blue light is at 4.35 mm to perform PDT at optimized results.

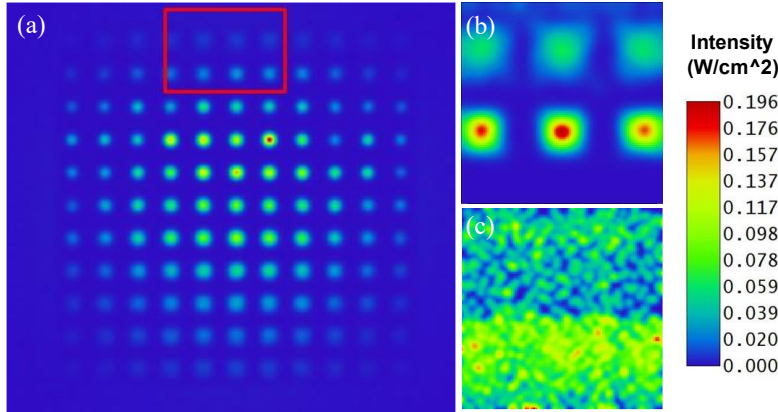


Fig. 8. (a) Detector display of the designed system for blue light at 2 mm inside the skin tissue. (b) Focused image of R1 and R2 at the epidermis. (c) Defocused image of R1 and R2 at 2.5 mm inside the skin tissue due to variable focal length.

The extended depth of field typically improves light delivery by increasing the appropriate depth. At a depth of 4.35 mm, the optical intensity at the tissue surface is approximately 36% of the input intensity, and it gradually decreases as the light penetrates deeper into the skin tissue. **Fig. 8a,b** show the detector display at a depth of 2 mm inside the skin tissue, with lenses at the R1 and R2 positions illuminating the epidermal layer and beyond. As the ray path becomes unfocused, the light becomes distorted, as shown in Fig. 8c, resulting in reduced power on the tissue. **Fig. 9a** depicts tunable illumination at a depth of 3.5 mm inside the skin tissue, and **Fig. 9b** shows the focused lighting onto the initial reticular dermal layers. **Fig. 10a** demonstrates illumination at the end of the dermal layer, where the light is focused by R10 and R11. In conclusion, this attempt at optical simulation has demonstrated improved light delivery into skin fold models.

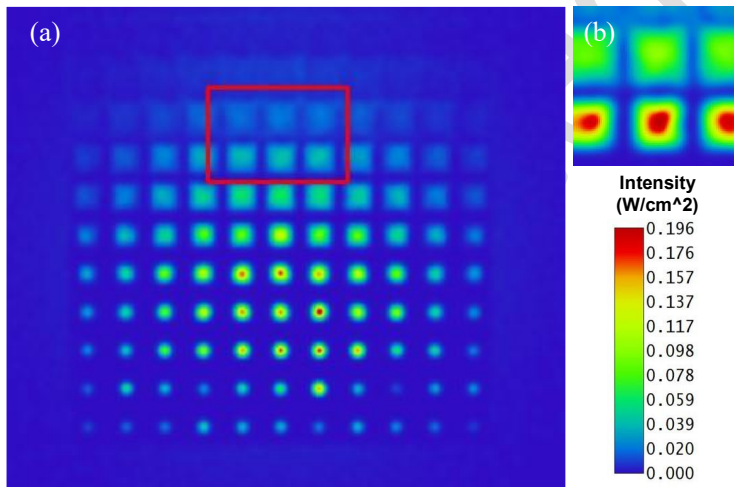


Fig. 9. (a) Detector display of the designed system for blue light at 3.5 mm inside the skin tissue. (b) Focused image of R3 and R4 at the reticular dermis.

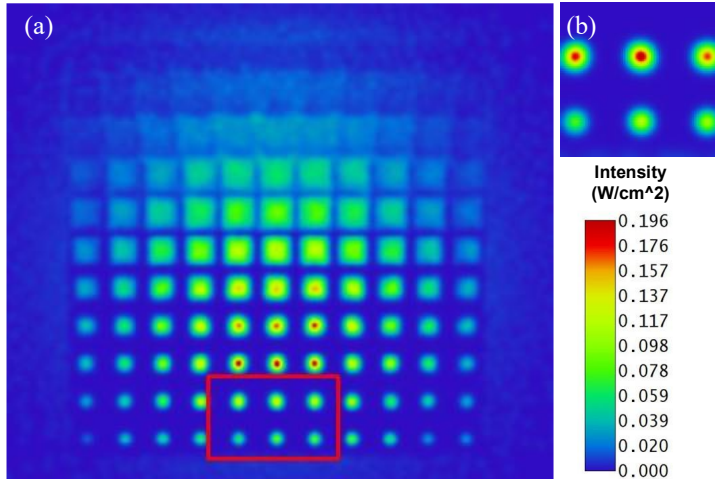


Fig. 10. (a) Detector display of the designed system for blue light at 4.2 mm inside the skin tissue. (b) focused image of R10 and R11 at the end of the dermal layer.

Red light is capable of penetrating deeper into the skin compared to other visible wavelengths due to its low absorption as it propagates through the skin tissue. Therefore, this property makes it an ideal candidate for various biomedical applications, including skin therapies and diagnostics. The optical penetration depth of red light targeted using tunable microlens integrated MNA array within the skin tissue is 6.5 mm, with an intensity of 13% of the input source. **Fig. 11** depicts the illumination of red light inside the skin tissue, demonstrating an enhanced penetration depth. This improved penetration allows for better visualization and targeting of specific structures within the skin, such as blood vessels and pigmented lesions.

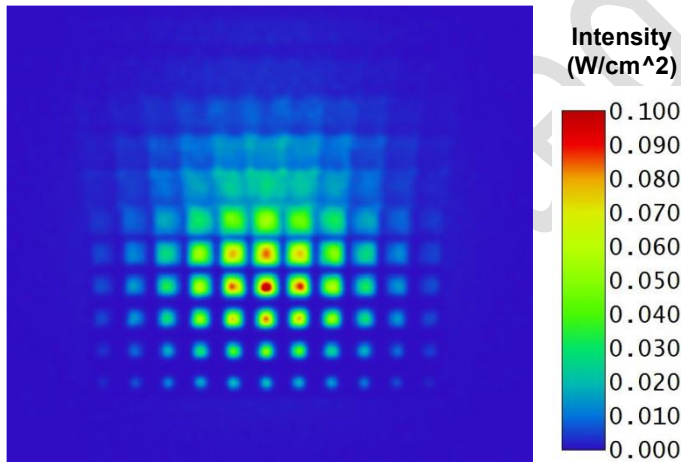


Fig. 11. Detector display of the designed system for red light at 6.5 mm inside the skin tissue.

5. Conclusion

Light has a tremendous number of therapeutic values which are very important for the treatment of skin cancers. One such example is photodynamic therapy, where a PS is injected into the body which gets activated at a certain wavelength after being absorbed by the tumor. This, as a result, causes a reduction of the tumor size through ROS production and cell necrosis. The scope of this paper includes:

- A tunable microlens integrated MNA has been developed with a variable focal length to increase the intensity and penetration depth of target areas. This design enables a target depth of up to 4.35 mm with 36% of the input intensity for blue light and up to 6.5 mm with 13% of the input intensity for red light.
- Development of the skin model is done to provide accurate simulation results of light penetration and irradiance inside the tissue.
- An optimization algorithm is also shown and applied.

- Furthermore, an in-depth analysis of tumor stages is also provided.

Although the current study focuses on optimizing the system to achieve variable light distribution at maximal intensity within a specific depth, the design parameters of the system can be tailored to meet specific requirements based on various factors, such as optical wavelength, tissue type, therapeutic depth range, and in-vitro applications. The proposed system can also be integrated with medical devices, such as endoscopes. For instance, if necessary, the optical microneedle array can be attached to a fiber optical probe for coupled laser PDT in interstitial application. By extending the effective therapeutic depth, this device can be widely utilized to enhance the efficacy of existing phototherapies, including blue light therapy for antimicrobial treatment and photodynamic therapy for different types of cancerous lesions inside the body. With the help of state-of-the-art fabrication techniques, the implementation of such a scheme would give enhanced optical performance for modern biomedical applications in light delivery systems.

Declaration of conflicting interests

The authors declare that they have no known competing financial interests or personal relationships that could have appeared to influence the work reported in this paper.

References

- Abrahamse, H., & Hamblin, M. R. 2016. "New photosensitizers for photodynamic therapy". *Biochemical Journal*, 473(4), 347-364.
- Allen, D. C. (2000). *Histopathology reporting*: Springer.
- Ash, C., Dubec, M., Donne, K., & Bashford, T. 2017. "Effect of wavelength and beam width on penetration in light-tissue interaction using computational methods". *Lasers in medical science*, 32, 1909-1918.
- Calixto, G. M. F., Bernegossi, J., De Freitas, L. M., Fontana, C. R., & Chorilli, M. 2016. "Nanotechnology-based drug delivery systems for photodynamic therapy of cancer: a review". *Molecules*, 21(3), 342.
- Eggermont, A. M., Chiarion-Sileni, V., Grob, J. J., Dummer, R., Wolchok, J. D., Schmidt, H., . . . Richards, J. M. (2014). Ipilimumab versus placebo after complete resection of stage III melanoma: Initial efficacy and safety results from the EORTC 18071 phase III trial. In: American Society of Clinical Oncology.
- Ganeson, K., Alias, A. H., Murugaiyah, V., Amirul, A.-A. A., Ramakrishna, S., & Vigneswari, S. 2023. "Microneedles for Efficient and Precise Drug Delivery in Cancer Therapy". *Pharmaceutics*, 15(3), 744.
- Guo, C., Yu, H., Feng, B., Gao, W., Yan, M., Zhang, Z., . . . Liu, S. 2015. "Highly efficient ablation of metastatic breast cancer using ammonium-tungsten-bronze nanocube as a novel 1064 nm-laser-driven photothermal agent". *Biomaterials*, 52, 407-416.
- He, X., Chen, Y., & Tang, L. (2008). *Modeling of flexible needle for haptic insertion simulation*. Paper presented at the 2008 IEEE Conference on Virtual Environments, Human-Computer Interfaces and Measurement Systems.
- Iqbal, A., Biermann, D., Ali, H. M., Zaini, J., & Metzger, M. 2019. "Investigating the impact of tool inertia on machinability of a β -titanium alloy using tool deflection and acoustic emission". *Proceedings of the Institution of Mechanical Engineers, Part B: Journal of Engineering Manufacture*, 233(7), 1745-1760.
- Jiang, Z., Shao, J., Yang, T., Wang, J., & Jia, L. 2014. "Pharmaceutical development, composition and quantitative analysis of phthalocyanine as the photosensitizer for cancer photodynamic therapy". *Journal of pharmaceutical and biomedical analysis*, 87, 98-104.
- Keung, E. Z., & Gershenwald, J. E. 2018. "The eighth edition American Joint Committee on Cancer (AJCC) melanoma staging system: implications for melanoma treatment and care". *Expert review of anticancer therapy*, 18(8), 775-784.
- Khatri, N., Berwal, S., Manjunath, K., & Singh, B. 2023. "Optical design and fabrication of zinc selenide microlens array with extended depth of focus for biomedical imaging". *Nanofabrication*, 8.
- Kim, M., An, J., Kim, K. S., Choi, M., Humar, M., Kwok, S. J., . . . Yun, S. H. 2016. "Optical lens-microneedle array for percutaneous light delivery". *Biomedical optics express*, 7(10), 4220-4227.
- Kim, M. M., & Darafsheh, A. 2020. "Light sources and dosimetry techniques for photodynamic therapy". *Photochemistry and photobiology*, 96(2), 280-294.
- Li, X., Zhao, Z., Zhang, M., Ling, G., & Zhang, P. 2022. "Research progress of microneedles in the treatment of melanoma". *Journal of Controlled Release*, 348, 631-647.
- Magnain, C., Elias, M., & Frigerio, J.-M. 2008. "Skin color modeling using the radiative transfer equation solved by the auxiliary function method: inverse problem". *JOSA A*, 25(7), 1737-1743.

- Marghoob, A. A., Koenig, K., Bittencourt, F. V., Kopf, A. W., & Bart, R. S. 2000. "Breslow thickness and Clark level in melanoma: support for including level in pathology reports and in American Joint Committee on Cancer Staging". *Cancer*, 88(3), 589-595.
- Naidoo, C., Kruger, C. A., & Abrahamse, H. 2018. "Photodynamic therapy for metastatic melanoma treatment: A review". *Technology in cancer research & treatment*, 17, 1533033818791795.
- Okuno, T., Kato, S., Hatakeyama, Y., Okajima, J., Maruyama, S., Sakamoto, M., . . . Kodama, T. 2013. "Photothermal therapy of tumors in lymph nodes using gold nanorods and near-infrared laser light". *Journal of controlled release*, 172(3), 879-884.
- Oltulu, P., Ince, B., Kokbudak, N., Findik, S., & Kilinc, F. 2018. "Measurement of epidermis, dermis, and total skin thicknesses from six different body regions with a new ethical histometric technique". *Turkish Journal of Plastic Surgery*, 26(2), 56.
- Paluncic, J., Kovacevic, Z., Jansson, P. J., Kalinowski, D., Merlot, A. M., Huang, M. L.-H., . . . Richardson, D. R. 2016. "Roads to melanoma: Key pathways and emerging players in melanoma progression and oncogenic signaling". *Biochimica et Biophysica Acta (BBA)-Molecular Cell Research*, 1863(4), 770-784.
- Robinson, J. T., Welsher, K., Tabakman, S. M., Sherlock, S. P., Wang, H., Luong, R., & Dai, H. 2010. "High performance in vivo near-IR (> 1 μm) imaging and photothermal cancer therapy with carbon nanotubes". *Nano research*, 3, 779-793.
- Ruiz-González, R., Acedo, P., Sánchez-García, D., Nonell, S., Cañete, M., Stockert, J. C., & Villanueva, A. 2013. "Efficient induction of apoptosis in HeLa cells by a novel cationic porphycene photosensitizer". *European Journal of Medicinal Chemistry*, 63, 401-414.
- Sharman, W. M., Allen, C. M., & Van Lier, J. E. 1999. "Photodynamic therapeutics: basic principles and clinical applications". *Drug discovery today*, 4(11), 507-517.
- Singh, S., Aggarwal, A., Bhupathiraju, N. D. K., Arianna, G., Tiwari, K., & Drain, C. M. 2015. "Glycosylated porphyrins, phthalocyanines, and other porphyrinoids for diagnostics and therapeutics". *Chemical reviews*, 115(18), 10261-10306.
- Sung, H., Ferlay, J., Siegel, R. L., Laversanne, M., Soerjomataram, I., Jemal, A., & Bray, F. 2021. "Global cancer statistics 2020: GLOBOCAN estimates of incidence and mortality worldwide for 36 cancers in 185 countries". *CA: a cancer journal for clinicians*, 71(3), 209-249.
- Swavey, S., & Tran, M. (2013). Porphyrin and phthalocyanine photosensitizers as PDT agents: a new modality for the treatment of melanoma. In *Recent Advances in the biology, therapy and management of melanoma*: IntechOpen.
- Wu, X., KONO, J., TAKAMA, N., & KIM, B. (2019). *Development of Optical Microlens-Microneedle Array for Phototherapy*. Paper presented at the Proceedings of JSPE Semestrial Meeting 2019 JSPE Spring Conference.
- Wu, X., Park, J., Chow, S. Y. A., Kasuya, M. C. Z., Ikeuchi, Y., & Kim, B. 2022. "Localised light delivery on melanoma cells using optical microneedles". *Biomedical optics express*, 13(2), 1045-1060.
- Wu, X., Takama, N., & Kim, B. (2019). *A biodegradable microneedles-trapezoidal micropatterned patch in the LED therapy*. Paper presented at the 2019 IEEE CPMT Symposium Japan (ICSJ).
- Yang, T. D., Park, K., Kim, H.-J., Im, N.-R., Kim, B., Kim, T., . . . Choi, Y. 2017. "In vivo photothermal treatment with real-time monitoring by optical fiber-needle array". *Biomedical optics express*, 8(7), 3482-3492.
- Zhao, H., Wang, X., Geng, Z., Liang, N., Li, Q., Hu, X., & Wei, Z. 2022. "Dual-function microneedle array for efficient photodynamic therapy with transdermal co-delivered light and photosensitizers". *Lab on a Chip*, 22(23), 4521-4530.
- Zhu, T. C., & Finlay, J. C. 2008. "The role of photodynamic therapy (PDT) physics". *Medical physics*, 35(7Part1), 3127-3136.



'Publisher's note: Eurasia Academic Publishing Group (EAPG) remains neutral with regard to jurisdictional claims in published maps and institutional affiliations.

Open Access This article is licensed under a Creative Commons Attribution-NoDerivatives 4.0 International (CC BY-ND 4.0) licence, which permits copying and redistributing the material in any medium or format for any purpose, even commercially. The licensor cannot revoke these freedoms as long as you follow the licence terms. Under the following terms you must give appropriate credit, provide a link to the license, and indicate if changes were made. You may do so in any reasonable manner, but not in any way that suggests the licensor endorsed you or your use. If you remix, transform, or build upon the material, you may not distribute the modified material.

To view a copy of this license, visit <https://creativecommons.org/licenses/by-nd/4.0/>.

Accepted version